Material Losses from TNI Coating Noise Measurements

ET-0010A-14

I. M. Pinto and the UniSannio ELiTES Team

on behalf of ELiTES WP2

Material Losses from TNI Coating Noise Measurements

I.M. Pinto and the UniSannio ELiTES Team

1.1 From Coating Noise to Coating Loss Angles. The Thermal Noise Interferometer

The thermal noise interferometer (henceforth TNI - see Figure 1) is a test-bed instrument designed to measure the thermal noise of dielectric mirror coatings (Black et al., 2004). The first instrument of this kind was described in (Numata et al., 2003). Conceptually similar instruments are presently under development at AEI (Westphal et al., 2012) and UFL (Eichholz et al., 2013).
Key features of the Caltech LIGO-Lab TNI (Black et al., 2004) used to make the measurements discussed in this paper are a frequency stabilized laser operating at 1064 nm, a small beam radius (164 μm), to enhance the effect of the fluctuations of the test mass surface, short test cavities, to reduce the laser frequency stabilization requirements, and twin test-cavities to permit common-mode noise rejection.
The power spectral density (henceforth PSD) of the coating Brownian noise can be written (Harry et al., 2006):

$$S_B(f) = \frac{2k_BT}{\pi^{3/2}f}\frac{(1-\sigma_s^2)}{wY_s}\phi_c, \tag{1.1}$$

where k_B is Boltzmann's constant, T is the absolute temperature, w is the effective (Gaussian) laser beam radius, σ_s is the Poisson's ratio of the substrate, and Y_s its Young's modulus. The noise PSD is accordingly proportional to the effective loss angle of the coating, ϕ_c.
Once a set of test mirrors is installed in the TNI, the noise floor of the instrument can be measured, and the effective loss angle of the coating can be obtained from a least-squares fit of the function

$$l(f) = \sqrt{4S_B(f) + S_s} \tag{1.2}$$

to the measured spectral density of noise, where $S_B(f)$ is given in Eq. (1.1), S_s is the power spectral density of shot noise, and the factor four comes from the fact that there are a total of four test mirrors in the twin cavities of the TNI.
The only free parameter in the fit is ϕ_c, since the shot noise can be measured independently (Black et al., 2004). The fit is performed using noise data taken between 2 and 4 kHz, which represents the core of the coating noise dominated band.
Using the above sketched procedure, the loss angles of four different coatings were measured at the TNI (Villar et al., 2011). The results are of interestive for the design of KAGRA, and will be accordingly summarized below.
The first coating was a standard quarter wavelength (QWL) stacked doublets design, using Silica and Tantala for the low and high index materials, respectively.
The second coating also used stacked doublets of Silica and Tantala, but the thickness of the layers and the number of doublets was adjusted so as to minimize thermal noise, while keeping the coating reflectivity at $1064nm$ unchanged. This "optimized" design is described in detail in (Villar et al., 2010).

Coating #	Type	Materials	Manufacturer
1	QWL	SiO_2/Ta_2O_5	REO
2	Optimized	SiO_2/Ta_2O_5	LMA
3	QWL	$SiO_2/TiO_2 :: Ta_2O_5$	LMA
4	Dichroic optimized.	$SiO_2/TiO_2 :: Ta_2O_5$	LMA

Table 1.1: The four different coatings whose loss angle was measured at TNI.

The third coating was a QWL design using Silica for the low index material and Tantala doped with Titania (to a concentration of $\sim 15\%$) for the high index material, which also reduces thermal noise (Harry et al., 2007).
Finally, the fourth coating was made from Silica and the same Titania-doped Tantala, and its noise was minimized using layer thickness optimization, but was designed for *dichroic* operation (featuring some reflectance at 532 nm also, needed for locking-acquisition in Advanced LIGO).
All coatings were deposited on fused silica substrates. The first was manufactured by Research Electro-Optics (REO) Inc.; the other three by Laboratoire des Materiaux Avances (LMA) of IN2P3.
The four coatings are summarized in Table 1.1.

1.2 From ϕ_c to Material Loss Angles

The effective loss angle of a coating, ϕ_c is a thickness (volume)-weighted average of the loss angles of its low and high index constituents (Villar et al., 2010), viz.

$$\phi_c = b_L d_L \phi_L + b_H d_H \phi_H, \tag{1.3}$$

where d_L and d_H are the total thickness of the low and high index materials, respectively, ϕ_L and ϕ_H their loss angles, and the coefficients $b_{L,H}$ are given by

$$b_{L,H} = \frac{1}{\sqrt{\pi} w} \left(\frac{Y_{L,H}}{Y_s} + \frac{Y_s}{Y_{L,H}} \right), \tag{1.4}$$

Y_s, Y_L and Y_H denoting the Young's moduli of the substrate, low index and high index material, respectively. In the limit of negligible Poisson ratios, Eq. (1.3) agrees well with the more complicated formulas derived in (Harry et al., 2006) from first principles.
Given two coatings, labeled (I) and (II), using the same materials but with different thicknesses, eqs. (1.3) yield

$$\mathbf{M} \cdot \phi = \phi_{\mathbf{c}}. \tag{1.5}$$

where

$$\phi = \begin{bmatrix} \phi_L \\ \phi_H \end{bmatrix}, \ \phi_{\mathbf{c}} = \begin{bmatrix} \phi_c^{(I)} \\ \phi_c^{(II)} \end{bmatrix}, \tag{1.6}$$

and

$$\mathbf{M} = \begin{bmatrix} b_L d_L^{(I)} & b_H d_H^{(I)} \\ b_L d_L^{(II)} & b_H d_H^{(II)} \end{bmatrix}. \tag{1.7}$$

The low and high index material loss angles are accordingly related to the loss angles of coatings I and II by the affine (in particular, linear) transformation,

$$\phi = \mathbf{M}^{-1} \cdot \phi_{\mathbf{c}}. \tag{1.8}$$

In (Villar et al., 2010) it was noted that the residuals of the fitting used to estimate the coating loss angles from the measured Brownian noise spectra are Gaussian distributed (see Figure 2). This allows us to model $\phi_c^{(I)}$ and $\phi_c^{(II)}$ in (1.8) as independent, Gaussian distributed random variables.
The estimated loss angles ϕ_c and the std. deviations σ_{ϕ_c} of their fitting residuals from (Villar et al., 2010) are collected in Table 1.2, for the four coatings in Table 1.1.

Coating #	estimated ϕ_c	std. deviation σ_{ϕ_c}
1	$8.4 \cdot 10^{-4}$	$0.3 \cdot 10^{-4}$
2	$6.9 \cdot 10^{-4}$	$0.2 \cdot 10^{-4}$
3	$6.0 \cdot 10^{-4}$	$0.5 \cdot 10^{-4}$
4	$5.5 \cdot 10^{-4}$	$0.25 \cdot 10^{-4}$

Table 1.2: TNI retrieved loss angles and related std. deviations for the coatings in Table 1.1.

Under these assumptions, in view of (1.8) ϕ_L and ϕ_H will be jointly Gaussian, and their distribution $\Psi_2(\phi_L, \phi_H)$ will be completely characterized by the average vector

$$\mathbf{M}^{-1} \cdot E\{\phi_{\mathbf{c}}\}, \tag{1.9}$$

and the covariance matrix (Papoulis, 2002)

$$\mathbf{M}^{-1} \cdot \begin{bmatrix} \sigma^2_{\phi_c^{(I)}} & 0 \\ 0 & \sigma^2_{\phi_c^{(II)}} \end{bmatrix} \cdot \left[\mathbf{M}^{-1}\right]^T. \tag{1.10}$$

The related *marginal* distributions of ϕ_L and ϕ_H, which are the sought quantities, will be accordingly given by

$$\Psi(\phi_L) = \int_{-\infty}^{\infty} d\phi_H \Psi_2(\phi_L, \phi_H), \quad \Psi(\phi_H) = \int_{-\infty}^{\infty} d\phi_L \Psi_2(\phi_L, \phi_H) \tag{1.11}$$

These are readily computed in closed analytic form and, being Gaussian, are completely characterized by their 1st and 2nd order moments.

1.2.1 Silica and Tantala Loss Angles

The mechanical loss angles of Silica and Tantala were estimated by applying the above sketched procedure to coatings #1 and #2 from Table 1.1.
To calculate the elements of $\mathbf{M}$ we use the fiducial values $Y_s = Y_{SiO_2} = 73$ GPa, and $Y_{Ta_2O_5} = 140$ GPa for the Young moduli, as customary throughout the topical Litrature, and the thickness values collected in Table 1.3 below.

Coating #	d_L $[\mu m]$	d_H $[\mu m]$
1	2.72	1.83
2	4.05	1.36
3	2.54	1.67
4	2.36	1.45

Table 1.3: Coating #1 and #2 material thicknesses.

The coating thickness uncertainties are of the order of a few nm, due to the high accuracy of the coating deposition process, and have no sensible effect on the retrieved material loss angles. On the other hand, as discussed in Section 1.4.6, the actual value of the Young moduli may be different from the fiducial values, depending on the thermal (annealing) treatment of the materials, by several percent.
The joint distribution of ϕ_{SiO_2} and $\phi_{Ta_2O_5}$ obtained from (1.9) and (1.10) is shown in Figure 3, (left panel) together with a few of its quantile-ellipses (right panel). These latter are *squeezed* along a line going through the point $\{E(\phi_L), E(\phi_H)\}$ where the distribution is peaked, with slope $\approx -.51$, reflecting the non-diagonal nature of the the matrix $\mathbf{M}^{-1}$ in 1.10, and the correlation between ϕ_L and ϕ_H.
The 1st and 2nd order moments of the derived (Gaussian) marginal distributions of ϕ_{SiO_2} and $\phi_{Ta_2O_5}$ are collected in Table 1.3 .
It is interesting to compare the confidence intervals obtained from the above reasoning, based on the observed Gaussianity of the coating loss angle fitting residuals, to the uncertainty intervals obtained from standard error propagation formulas, yielding

$$\Delta\phi = \mathrm{abs}(\mathbf{M}^{-1}) \cdot \Delta\phi_{\mathbf{c}} \tag{1.12}$$

where abs$(\cdot)$ applies the absolute value to all elements of its argument.
Error propagation is equivalent to the simple graphic construction shown in Figure 4, where in the $\{\phi_H, \phi_L\}$-plane one looks at the intersections the uncertainty *strips* obtained from eq. (1.4) upon letting $\phi_c = \phi_c^{(0)} \pm \Delta\phi_c$.
The uncertainty intervals obtained in this way upon letting $\Delta\phi_{\mathbf{c}} = \sigma_{\phi_c}$ are also listed in Table 1.3 below.

1.2.2 Titania Doped Tantala Loss Angle

For coatings #3 and #4 in Table I the matrix $\mathbf{M}$ turns out to be ill-conditioned, and the procedure described in Sect. 1.2.1 yields exceedingly broad confidence in-

Loss angle 95% c.i.	from marginal distribution	from error propagation
ϕ_{SiO_2}	$(0.514 \pm 0.3) \cdot 10^{-4}$	$(0.5 \pm 0.3) \cdot 10^{-4}4$
$\phi_{Ta_2O_5}$	$(4.722 \pm 0.562) \cdot 10^{-4}$	$(4.7 \pm 0.4) \cdot 10^{-4}$

Table 1.4: Silica and Tantala loss angles from coatings #1 and #2 .

tervals, in view of eq. (1.10).
If we make the reasonable assumption that the loss angle of the low-index material (Silica) is *the same* for all coatings in Table 1.1, the low index material being fiducially the same, we may derive *two* (independent) estimates for the loss angle of the high index material from the measured loss angles of coatings #3 and #4. Given that both the coating loss angles and the low-index material loss angle uncertainties are Gaussian distributed, the retrieved high-index loss angles will be also Gaussian distributed, with

$$E[\phi_H] = \frac{1}{b_H d_H} E[\phi_c] - \frac{b_L d_L}{b_H d_H} E[\phi_L], \tag{1.13}$$

$$\mathrm{var}[\phi_H] = \left(\frac{1}{b_H d_H}\right)^2 \mathrm{var}[\phi_c] + \left(\frac{b_L d_L}{b_H d_H}\right)^2 \mathrm{var}[\phi_L]. \tag{1.14}$$

The two distributions obtained from coatings #3 and #4 can be eventually combined (technically, pooled) to obtain a refined (technically, maximum-likelihood) distribution. This latter is also Gaussian, with 1st and 2nd order moments (Papoulis, 2002):

$$E[\phi_H] = w_I E[\phi_H]_I + w_{II} E[\phi_H]_{II}, \tag{1.15}$$

$$\mathrm{var}[\phi_H] = w_I^2 \mathrm{var}[\phi_H]_I + w_{II}^2 \mathrm{var}[\phi_H]_{II} \tag{1.16}$$

where

$$w_{I,II} = \frac{\mathrm{var}[\phi_H]_{I,II}^{-1/2}}{\mathrm{var}[\phi_H]_I^{-1/2} + \mathrm{var}[\phi_H]_{II}^{-12}}. \tag{1.17}$$

Similarly, retrieving the material loss angle confidence intervals from the intersections of the coating loss uncertainty-strips of coatings #3 and #4 in the $\{\phi_L, \phi_H\}$ plane yields extremely large uncertainties.
The std. error propagation formulas can be used in this case, by intersecting *each* of the coating loss uncertainty strips with the strip $\phi_L = E[\phi_L] \pm \sigma_{\phi_L}$, as shown in Figure 6, and *then* computing the intersection of the resulting uncertainty intervals for $\phi_{Ti::Ta_2O_5}$. The 1st and 2nd moment of the pooled distribution are collected in Table 1.5, together with the uncertainty intervals obtained upon letting $\Delta\phi_c = \sigma_{\phi_c}$.

1.3 Comparison with EMT Model

It is interesting to compare the above results to those obtained from mixture (aka effective medium) theory based approach. Despite their simplicity, effec-

Loss angle 95% c.i.	from pooled distributions	from error propagation
$\phi_{Ti::Ta_2O_5}$	$(3.66 \pm 0.56)\,10^{-4}$	$(3.6 \pm 0.5)\,10^{-4}$

Table 1.5: Ti-doped Tantala loss angle from coatings #1 and #2.

tive medium theories (henceforth EMT) admit a solid microscopic foundation (Aspnes, 1982), and have been widely and successfully used to model the optical (complex refraction index) and mechanical (e.g., elastic and bulk moduli) of composite materials. Their use has been accordingly proposed to model glassy mixtures for GW interferometer optical coatings (Pinto et al., 2011).

Here we shall adopt the well known Bruggemann approach (Bruggeman, 1935) which treats the host medium and the inclusions on equal grounds, assuming both to be embedded into an effective medium, and results into mixture formulas which are symmetric w.r.t. the host and inclusion params. The Bruggemann formula for the (complex) permittivity $\epsilon = n^2$ of a mixture is

$$\eta_2 \frac{\epsilon_2 - \epsilon_{mix}}{\gamma\epsilon_2 + (1-\gamma)\epsilon_{mix}} + (1-\eta_2)\frac{\epsilon_1 - \epsilon_{mix}}{\gamma\epsilon_1 + (1-\gamma)\epsilon_{mix}} = 0, \tag{1.18}$$

where η is the volume fraction, the suffixes $1, 2$ and mix denote the constituents and the composite, and γ depends on the morphology of the inclusions (here we shall tentatively adopt the value 1=3, appropriate to spherical inclusions). Using the fiducial values $n_{Ta_2O_5} = 2.03$, $n_{TiO_2} = 2.29$, and $n_{Ti::Ta_2O_5} = 2.07$, we may use (1.18) to retrieve the Titania fraction in the doped material, yielding $\eta = 0.16$, as shown in Figure 7 (top left panel). This value is close to the nominal one for the LMA Ti-doped Tantala used in the coating prototypes tested. In order to compute the viscoelastic properties of the mixture we shall adopt the physically neat formulation by Barta (Barta, 1994), according to which the (complex) mixture elastic (Young) modulus, Y, and Poisson ratio, σ,can be found by solving the system

$$\begin{cases} (1-\eta_2)\dfrac{X - X_1}{2X + (X_1/y_1)(\sigma_1+1)} + \eta_2\dfrac{X - X_2}{2X + (X_2/y_2)(\sigma_2+1)} = 0 \\ \\ (1-\eta_2)\dfrac{X/y - X_1/y_1}{2X + (X_1/y_1)(\sigma_1+1)} + \eta_2\dfrac{X/y - X_2/y_2}{2X + (X_2/y_2)(\sigma_2+1)} = 0 \end{cases}, \tag{1.19}$$

where (omitting the subscripts for notational ease)

$$X = \frac{\sigma Y}{\sigma + 1}, y = \sigma - 2. \tag{1.20}$$

Equations (1.19) and (1.20) can be used to compute the Young's modulus and Poisson ratio of doped Tantala, using the fiducial values $Y_{Ta_2O_5} = 140$ GPa, $Y_{TiO_2} = 165$ GPa, $\sigma_{Ta_2O_5} = 0.23$, and $\sigma_{TiO_2} = 0.28$.
The real part of the mixture Young's modulus and Poisson ratio of the mixture (top right and bottom right panels in Figure 7) show no sensible dependence

on the (very small) constituents' loss angles. The loss angle (imaginary part of the elastic modulus) depends on the loss angle of the Tantala and Titania constituents as shown in the bottom left panel of Figure 7.
We next attempt to compute a confidence interval for the Titania-doped Tantala loss angle, computed via EMT eqs. (1.19), (1.20), assuming for the Tantala loss angle a (Gaussian) distribution obtained from the TNI measurements on undoped coatings, and for the Titania loss angle a Gaussian distribution, with average value 1.2 10^{-4} taken from (Scott and MacKrone, 1968), and a reasonable value for the standard deviation of 10% its average value. The Titania volume fraction is taken to be 16%, as obtained above via Bruggeman's formula.
The EMT deduced Ti-doped Tantala loss angle distribution is shown in Figure 8, where it is compared with the distribution obtained from the measurements on coatings #3 and #4. The two distributions look fairly consistent.

1.4 Discussion and Conclusions

During the last decade the mechanical loss angle of various candidate coating materials for interferometric GW detectors have been estimated by several research Groups, both at room and cryogenic temperatures, from the measured damping-times of mechanical oscillators consisting of thin/thick disk or cantilever shaped blades, before and after coating deposition.
We include a brief summary of available room temperature results (mostly referring to ion-beam sputtered coatings), for comparison.

1.4.1 Suspended Disk Blades

A measurement setup based on suspended disk-shaped thin or thick blades was described in (Crooks et al. (2002), Harry et al. (2002)), and used to estimate the mechanical losses of several glassy oxides. Knowledge of the mechanical and optical losses of candidate materials led to downselect Silica (SiO_2) and Tantala (Ta_2O_5) as the "best" low and high index materials available for interferometric gravitational wave detector mirror coatings (Crooks et al., 2006). The main results obtained using this setup were summarized in (Penn et al., 2003), where it was notably argued that noise originates mainly from the coating bulk (the interfacial contributions being negligible), and the following estimates for the loss angles of annealed SiO_2 and (undoped) Ta_2O_5 were given $\phi_L = (0.5 \pm 0.3) \cdot 10^{-4}$ and $\phi_H = (4.4 \pm 0.2) \cdot 10^{-4}$, at frequencies of a few KHz.

1.4.2 Clamped Cantilevers

A different setup, based on clamped cantilever-shaped blades was developed at LMA, in collaboration with researchers from the Universities of Perugia and

Glasgow. An analytic model of the cantilever oscillator allowing to extract the coating loss angles from the measured quality factors was laid out in (Pierro and Pinto, 2006) for single-layer coatings, and in (Comtet et al., 2007) for the multi-layer ones.
This setup was used to estimate the loss angle of cantilevers coated with a single-layer of Silica or (undoped) Tantala, at frequencies $\sim 10^2 Hz$, yielding $\phi_L = (0.5 \pm 0.018) \cdot 10^{-4}$ and $\phi_H = (3.02 \pm 0.11) \cdot 10^{-4}$, respectively (Comtet et al., 2007).
The same setup was used at LMA to optimize *mixtures* where Tantala was doped with different materials (including Cobalt, Tungsten and Titan), to reduce its mechanical losses (Comtet et al., 2007). It was found that Ta_2O_5 doped with Ti at concentrations $\approx 14\%$ was on a par with undoped Tantala in terms of optical absorption, but better by $\approx 17\%$ in terms of loss angle. A similar reduction in loss angle going from plain to Ti-doped Tantala was observed also using a suspended disk Q-measurement setup (Harry et al., 2007), and also from TNI measurements on prototype mirrors with $SiO_2/Ti :: Ta_2O_5$ coatings. Experiments on other doped oxides (in particular ZrO_2) eventually indicated that Ti-doped Tantala was the best option for the high index material (Flaminio et al., 2010).
Repeated cantilever based mesurements from several groups produced consistent results for the Silica and Ti-doped Tantala loss angles (Flaminio et al., 2013), yielding: $\phi_L = (4.6 \pm 0.1) \cdot 10^{-5}$ and $\phi_{H^*} = (2.4 \pm 0.4) \cdot 10^{-4}$.

1.4.3 Multi-Layer Coated Cantilevers

Loss angle measurements on *multi*-layer coated cantilevers started around 2009. Coating loss angles *larger* than expected from single-layer results were obtained. The origin of the observed excess noise is, as yet, unclear.
Assuming $\phi_{H^*} = (2.4 \pm 0.2) \cdot 10^{-4}$, the multi-layer measurements yield $\phi_L = (1.3 \pm 0.4) \cdot 10^{-4}$, pretty larger than the value ($\approx 5 \cdot 10^{-5}$) retrieved from single-layer Silica coated blades (Flaminio et al., 2011). On the other hand, assuming $\phi_L \approx 0.5 \cdot 10^{-4}$, the same multi-layer blade measurements yield $\phi_H = (4.2 \pm 0.2) \cdot 10^{-4}$, pretty larger than the value ($\approx 2.4 \cdot 10^{-4}$) retrieved from single-layer Ti-doped Tantala coated blades (Flaminio et al., 2011).
Measurements at LMA indicated that excess noise was increasing with the number of layers (Flaminio et al., 2011), suggesting that excess losses could originate at the interfaces between the high and low index layers. But this is contradicted by already mentioned previous results, based on suspended multi - layer coated disk measurements in (Penn et al., 2003).
It was also suggested that interfacial diffusion during the annealing phase, producing graded/index regions at the boundaries between the low and high index layers, might account for the observed discrepancy (Cagnoli et al., 2012). A subsequent analysis based on EMT shew that interfacial diffusion is not enough to contribute the observed extra noise (Pinto et al., 2012).
It was recently observed that the distribution of the loss-angle fitting residuals

is usually markedly non-Gaussian for cantilever-based measurements (Principe and Pinto, 2014). Robust estimation of the retrieved loss-angle confidence intervals would be accordingly in order, possibly mitigating the discrepancies between loss angle estimates based on *single*-layer and *multi*-layer blades.

1.4.4 The Gentle Nodal Suspension

The accuracy and repeatability of clamped-cantilever based measurement is severely affected by clamping losses. Reducing these latter requires careful control of the contacting surfaces of the clamping-vise and cantilever (Flaminio et al., 2013). These problems can be mostly eliminated using a different setup, where a disk-shaped (thin or thick) blade is supported at a nodal point of its mechanical vibration pattern by a conical tip, ideally without friction (Cesarini et al., 2009).
Ringdown measurements of single-layer undoped Tantala-coated silicon disks, based on this setup (nicknamed *GeNS*, for *Ge*ntle *N*odal *S*uspension) yield loss angle values $\phi_H = (3.8 \pm 0.5) \cdot 10^{-4}$, with very good repeatability (Cesarini et al., 2009).

1.4.5 QDPI Cantilever Noise Measurement

A different measurement setup for the direct broadband measurement of thermal noise of coated cantilevers based on quadrature phase differential interferometry (QPDI, Paolino et al. (2013)) has been described in (Li et al., 2013).
The loss angles of SiO_2 and undoped Ta_2O_5 estimated from these measurements were $\phi_L = (6.2 \pm 0.05) \cdot 10^{-5}$ and $\phi_H = (4.7 \pm 0.07) \cdot 10^{-4}$, close to our TNI based results. Measurements on Ti-doped Tantala are underway.

1.4.6 Young Modulus

Retrieving the material loss angles from the measured loss angles of disks/blades before and after coating requires knowledge of the ratio between the energies stored in the coating and substrate, known as the energy dilution factor (Penn et al. (2003), Pierro and Pinto (2006), Comtet et al. (2007), Li et al. (2013)). This latter, can be expressed in terms of the of the tensile (Young) moduli of the substrate and coating materials [1]. The fiducial estimates $Y_L = 72.7\ GPa$ and $Y_H = 140\ GPa$, for Silica and (Ti-doped as well as undoped) Tantala, respectively, from popular optical glass databases, have been widely adopted so far. Accurate values of the Young moduli are also needed for retrieving material loss angles from TNI measurements.
Recent measurements of the Young modulus based both on nano-indentation (Abernathy, 2013) and ultrasonic reflection techniques (Rhoades et al. 2012) are ongoing. Preliminary results in (Abernathy et al., 2014) indicate that the Young modulus for Ti-doped Tantala may vary in a rather wide range (roughly from

[1] In (Li et al., 2013) an (accurate) approximate formula for the dilution factor in terms of the resonant frequencies and the linear mass density of the coated and uncoated blades is given.

120 to 175 Gpa) depending on Ti concentration and heat treatment.

1.4.7 Conclusions

On the basis of available results, the following conclusions can be drawn. Measurement of the Young modulus and mechanical losses of glassy oxides is a relatively recent research topic, no older than twelve years.
Experimental setups for material loss angle measurements have been steadily improving, resulting into better and better accuracy and repeatability.
Nonetheless, as of today, loss angle estimates from different measurement setups are not fully consistent. In particular, ringdown measurements on single-layer coated cantilevers are not consistent with those from multi-layer coated cantilevers, nor with those from TNI measurements on multi-layer coated mirrors. The reason of such discrepancies is yet unclear. A number of possible causes have been scrutinized so far, with little or no success.
Ongoing efforts toward more accurate knowledge of the relevant process/dependent material parameters (in particular, the Young modulus), and improved coating-noise models will certainly help clarifying this important issue.

Bibliography

M. Abernathy, 2013, "Introduction to Nano-Indentation," LIGO Document G1300976.

M. Abernathy et al., 2014, "Investigation of the Youngs Modulus and Thermal Expansion of Amorphous Titania-doped Tantala Films,"arXiv:1401.7061.

D.E. Aspnes, 1982, "Local Field Effects and Effective-Medium Theory: A Microscopic Perspective," Am. J. Phys. **50**, 704.

S. Barta, 1994, "Effective Young Modulus and Poisson's Ratio for the Particulate Composite," J. Appl. Phys. **75**, 3258.

E. D. Black et al., 2004, "Direct Observation of Broadband Coating Thermal Noise in a Suspended Interferometer," Phys. Lett. **A328**, 1.

D. A. G. Bruggeman, 1935, "Berechnung verschiedener physikalischer Konstanten von heterogenen Substanzen. I. Dielektrizittskonstanten und Leitfhigkeiten der Mischkrper aus isotropen Substanzen," Ann. Phys. **24**, 637.

D.G. Cacuci, 2004, *"Sensitivity Analysis and Uncertainty Theory,"* Chapman & Hall / CRC.

G. Cagnoli et al., 2012, "Coating Research and Development at LMA," GWADW 2012 presentation, LIGO DOcument G1200618.

E. Cesarini et al., 2009, "A Gentle Nodal Suspension for Measurements of the Acoustic Attenuation in Materials," Rev. Sci. Instr. **80**, 053904.

Ch. Comtet et al., 2007, "Reduction of Tantala Mechanical Losses in Ta_2O_5/SiO_2 Coatings for the Next Generation of VIRGO and LIGO Interferometric Gravitational Waves Detectors," 42th Rencontres de Moriond, Gravitational Waves and Experimental Gravity, La Thuile, http://hal.in2p3.fr/docs/00/17/75/78/PDF/Conf3.pdf.

D.R.M. Crooks et al., 2002, "Excess Mechanical Loss Associated with Dielectric Mirror Coatings on Test Masses in Interferometric Gravitational Wave Detectors," Class. Quantum Grav., **19**, 883.

D.R.M. Crooks et al., 2006, "Experimental Measurements of Mechanical Dissipation Associated with Dielectric Coatings Formed Using SiO_2, Ta_2O_5 and Al_2O_3," Class. Quantum Grav. /bf 23, 4593.

J. Eichholz, 2013, "Direct Measurement of Coating Thermal Noise with THOR: Progress and Cryogenic Implementation," LIGO Document G1301008.

R. Flaminio et al., 2010, "A Study of Coating Mechanical and Optical Losses in view of Reducing Mirror Thermal Noise in Gravitational Wave Detectors," Class. Quantum Grav. **27**, 084030.

R. Flaminio et al., 2011, "Coating R & D for Future GW Detectors," Amaldi 9 presentation, http://www.amaldi9.org/abstracts/420/Flaminio _Amaldi _2011 _July11.pdf .

R. Flaminio et al., 2013, "Characterization and Direct Thermal Noise Measurement of Coatings," GWADW 2013 presentation, Elba.

G.M. Harry et al., 2002, "Thermal Noise in Interferometric Gravitational Wave Detectors due to Dielectric Optical Coatings," Class. Quantum Grav., **19**, 897.

G.M. Harry et al. 2006, "Thermal Noise from Optical Coatings in GW Detectors," *Applied Optics*, **45**, 1569.

G.M. Harry et al. 2007, "Titania Doped Tantala/Silica Coatings for Gravitational Wave Detection," *Class. Quantum Grav.*, **24**, 405.

T. Li et al., 2013, "Measurements of Mechanical Thermal Noise and Energy Dissipation in Optical Dielectric Coatings," preprint ArXiv:1401.0184v1.

K. Numata et al., 2003, "Wide-Band Direct Measurement of Thermal Fluctuations in an Interferometer," Phys. Rev. Lett. **91**, 260602.

P. Paolino et al., 2013, "Quadrature Phase Interferometer for High Resolution Force Spectroscopy", Rev. Sci. Instrum. **84**, 095001.

A. Papoulis, 2002, *"Probability, Random, Variables and Stochastic Processes,"* New York, McGraw-Hill.

S.D. Penn et al. 2003, "Mechanical Loss in Tantala/Silica Dielectric Mirror Coatings," *Class. Quantum Grav.*, **20**, 2917.

V. Pierro and I.M. Pinto, 2006, "Measuring Coating Mechanical Quality Factors in a Layered Cantilever Geometry: a Fully Analytic Model," LIGO Technical Document T060173.

I.M. Pinto et al., 2011, "Effective Medium Theory for Modeling Dielectric Mixture Properties," LIGO Document G1100372.

I.M. Pinto et al., 2012, "Interdiffused Coatings," LIGO Document G1200976.

M. Principe and I.M. Pinto, 2014, work in progress.

E. Rhoades et al., 2012, "Ultrasonic Measurements of Youngs Modulus of LIGO Coatings," LIGO Document G1200796.

W.W. Scott and R.K. MacKrone, 1968, "Apparatus for Mechanical Measurements in Low Loss Materials at Audio frequencies and Low Temperatures," Rev. Sci. Instr., **39**, 821.

A.E. Villar et al., 2010, "Measurement of Thermal Noise in Multilayer Coatings with Optimized Layer Thickness "Phys. Rev. D **81**, 122001.

A.E. Villar et al., 2011, "Material Loss Angles from Direct Measurements of Broadband Thermal Noise: Statistical Analysis and Preliminary Comparison with Results from Mixture Theory," LIGO Document G1101096.

T. Westphal et al., 2012, "(Coating) Thermal Noise Interferometer," LIGO Document G1200560.

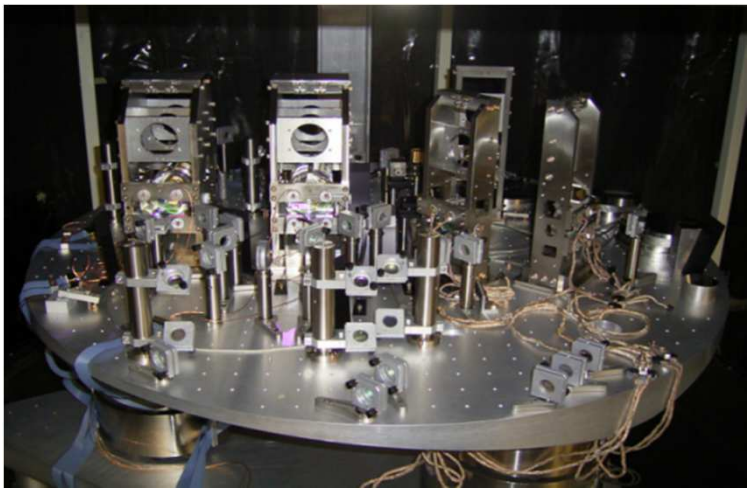

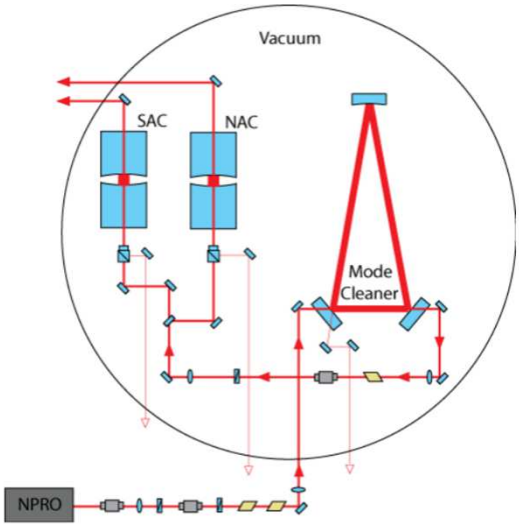

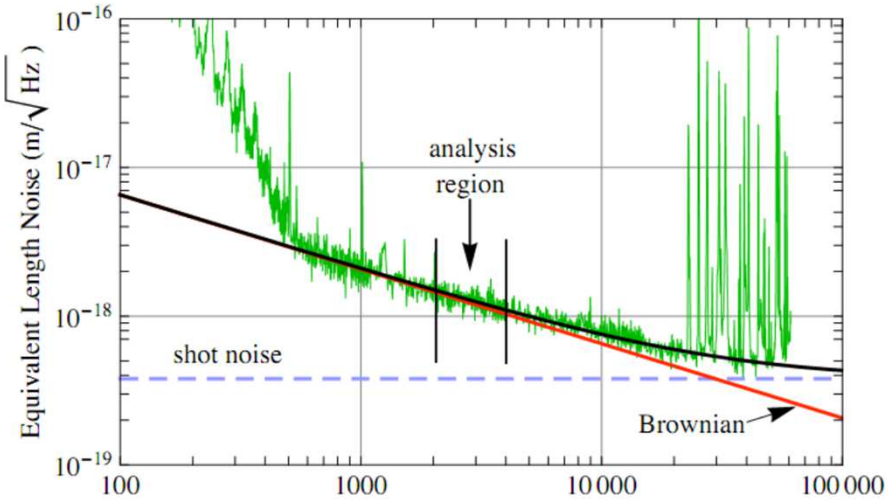

Figure 1 – Thermal Noise Interferometer bench (top), functional diagram (mid) and typical measured noise spectra (bottom) from (Villar et al., 2010).

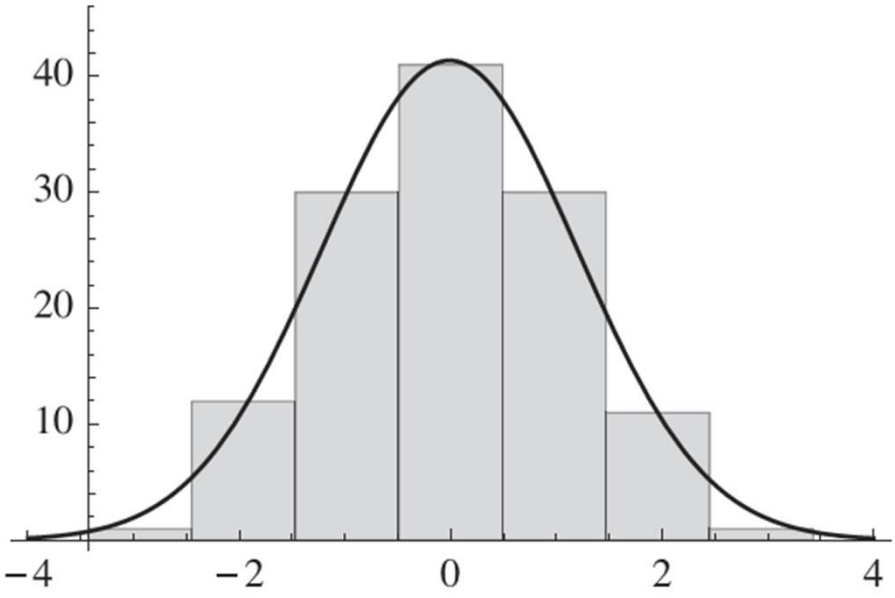

Figure 2 – Typical TNI coating loss angle fitting residual histogram (from Villar et al., 2010).

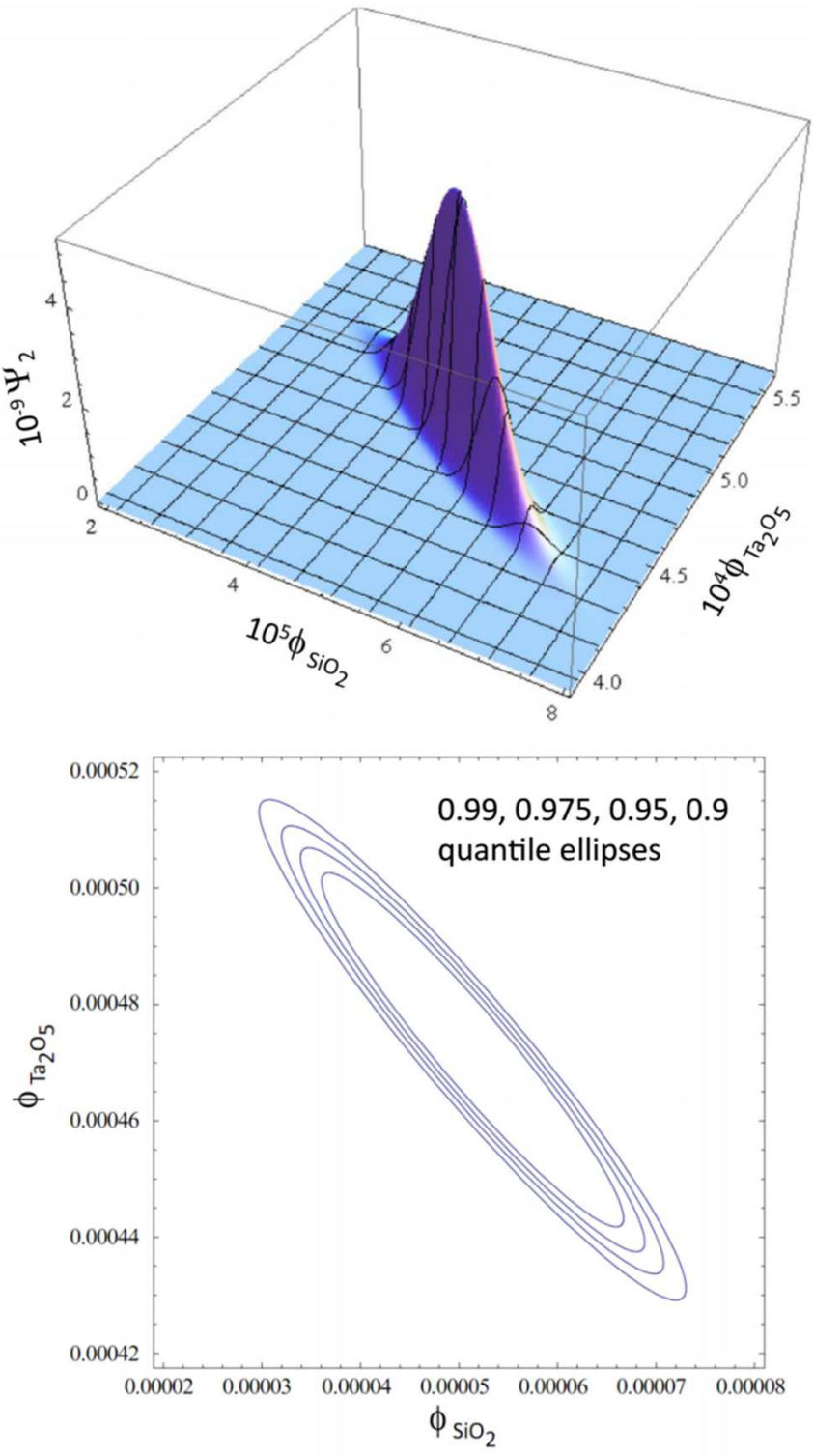

Figure 3 – Jointly Gaussian distribution of SiO_2 and Ta_2O_5 loss angles (top) from TNI measurements of coatings #1 and #2, and some of its quantile ellipses (bottom) from (Villar et al., 2011)

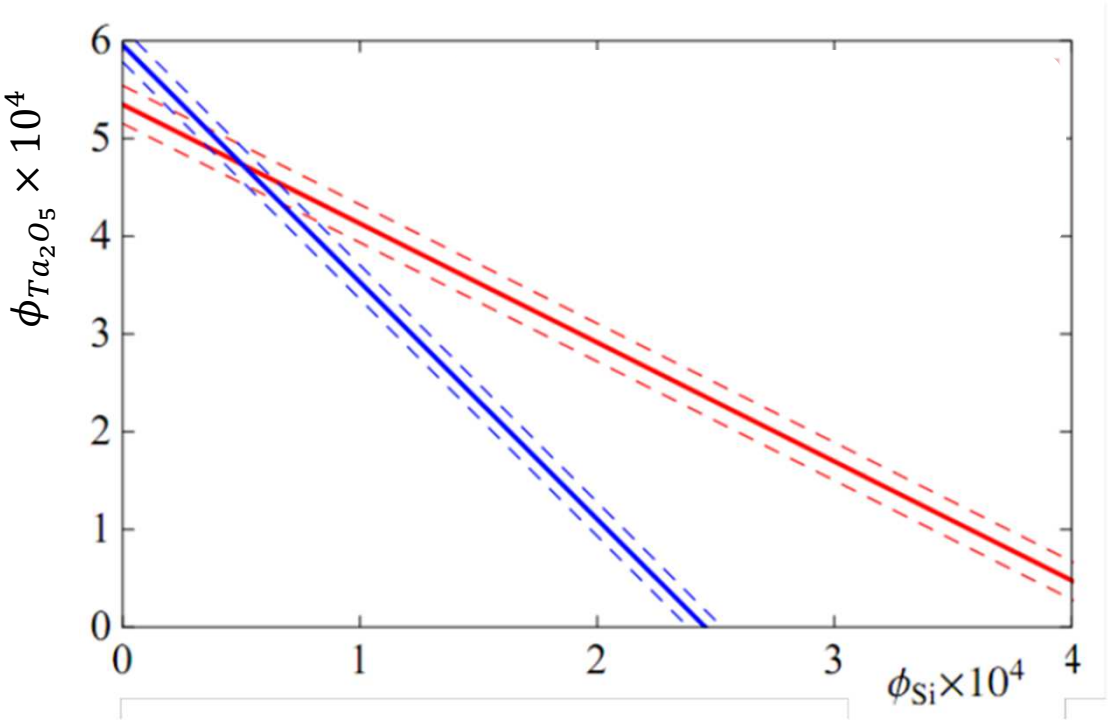

Figure 4 – Confidence intervals from error propagation for coatings #1 and #2 from (Villar et al., 2011).

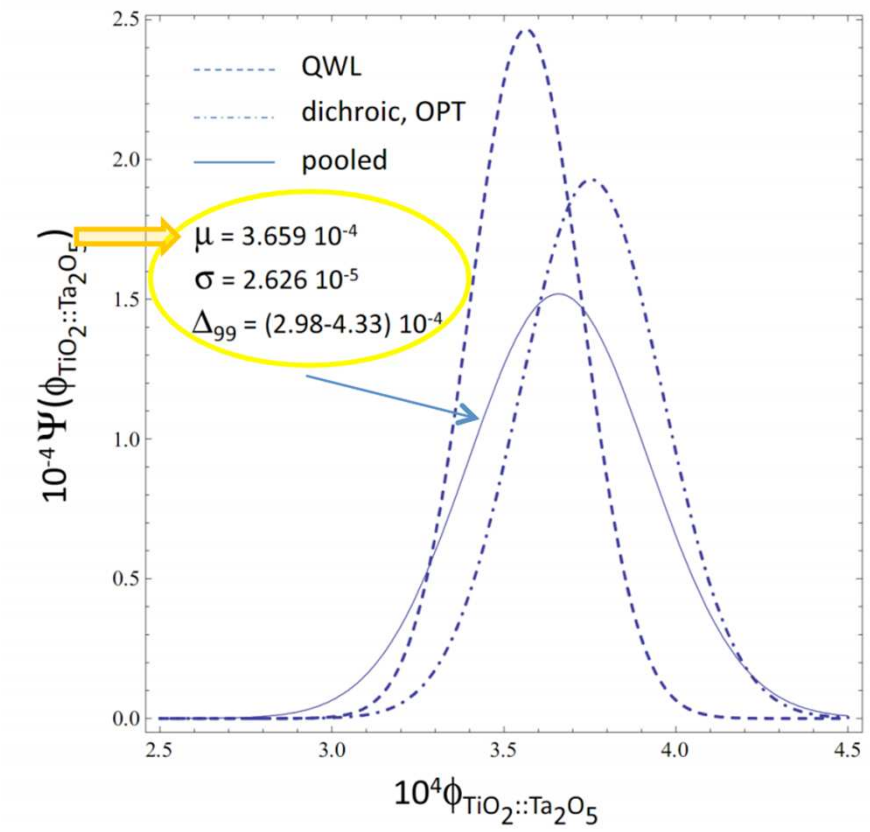

Figure 5 – Pooled distribution of TiO_2 :: Ta_2O_5 loss angle from (Villar et al., 2011)

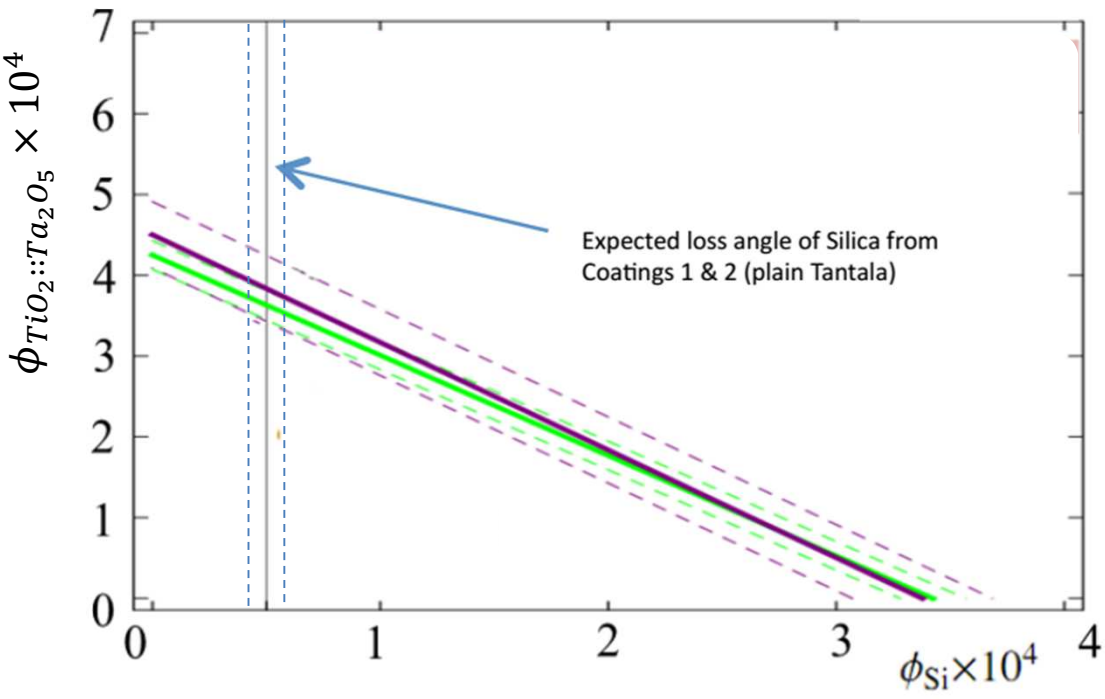

Figure 6 – Confidence interval from error propagation
for coatings #3 and #4 from (Villar et al., 2011).

.

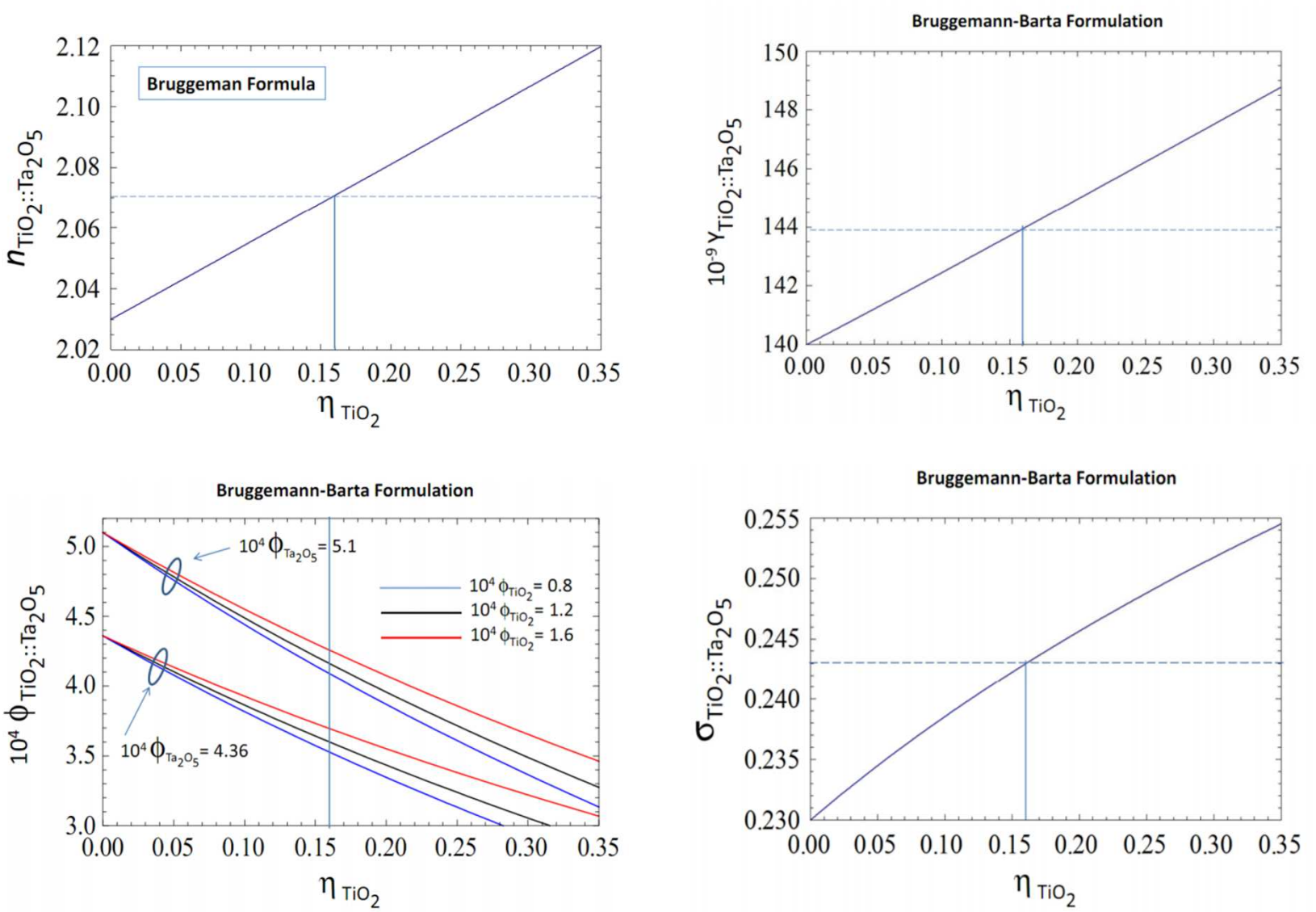

Figure 7 – Optical and viscoelastic parameters of Titania doped Tantala from EMT (Bruggemann-Barta) formulas. Top left: refraction index; top right: Young nodulus; bottom left mechanical loss angle; bottom right: Poisson modulus. from (Villar et al., 2011)

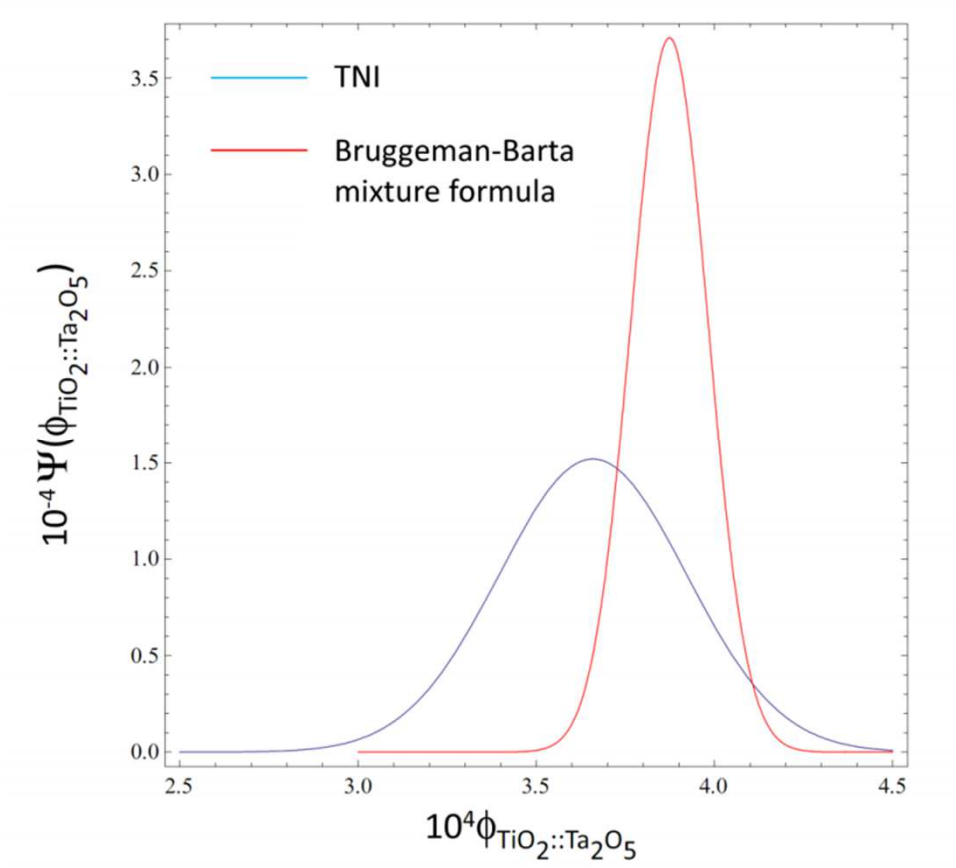

Figure 8 – Titania doped Tantala loss angle – comparison between TNI retrieved distribution and Bruggemann-Barta EMT formula with $\phi_{TiO_2} = (1.2 \pm 0.12) \cdot 10^{-4}$ from (Villar et al., 2011)